Collision-Induced Fine-Structure Transitions of $Hg(6^3P_1 \rightarrow 6^3P_0)$ with N_2 and CO. 2. Translational Energy Dependence

Misaki Okunishi,* Junichi Hashimoto, Hisashi Chiba, Kenji Ohmori, Kiyoshi Ueda, and Yukinori Sato

Research Institute for Scientific Measurements, Tohoku University, Katahira, Sendai, 980-8577, Japan

Received: October 26, 1998; In Final Form: January 13, 1999

Translational energy dependences of relative cross sections for $Hg(6^3P_1 \rightarrow 6^3P_0)$ fine-structure changing collisions with N_2 and CO have been measured with a crossed-beam apparatus over the energy range between 800 and 3750 cm^{-1}. A negative energy dependence is obtained for Hg−CO, but a positive energy dependence is observed for Hg−N_2, with an energy threshold for appearance of $Hg(6^3P_0)$ around 900 cm^{-1}. These results are explained using the characteristics of the intermolecular potentials for Hg−N_2 and Hg−CO. The existence of the energy threshold around 900 cm^{-1} for N_2 suggests simultaneous vibrational excitation of N_2. The translational energy dependence has also been measured under beam-gas conditions over the energy range between 450 and 3350 cm^{-1}. From a comparison with $Hg(6^3P_1 \rightarrow 6^3P_0)$ intramultiplet deactivation cross sections for Hg−N_2 and Hg−CO obtained in gas cell experiments, absolute values of the cross sections for this intramultiplet transition are estimated as a function of the average translational energy under the beam-gas conditions. There is no clear threshold for Hg−N_2 in the beam-gas experiment and it is suggested that a higher rotational temperature of N_2 induces a shift of the energy threshold effectively lower.

I. Introduction

Numerous experimental studies have been performed to investigate quenching of photoexcited $Hg(6^3P_1)$ atoms by various molecules[1−13] and the quenching cross sections have been determined from attenuation of fluorescence at 253.7 nm ($6^3P_1 \rightarrow 6^1S_0$) as a function of the pressure of target molecules.[1−7] An intramultiplet fine-structure transition,

$$Hg(6^3P_1) + M \rightarrow Hg(6^3P_0) + M^{\#} \times (\Delta E(^3P_1 - ^3P_0) = 1767\ cm^{-1}) \quad (1)$$

is one important pathway for the quenching of the $Hg(6^3P_1)$, because it produces metastable $Hg(6^3P_0)$, which can induce subsequential chemical reactions.[1−3,8,9] Partial cross sections for this intramultiplet transition have also been measured for various gas targets at room temperature.[10] Among them, intramultiplet transitions with two diatomic quenchers, N_2 and CO, attract special attention, because these two diatomic molecules are isoelectronic molecules with the same mass number and similar polarizability but the cross section for Hg−CO is about thirty times larger than that for Hg−N_2,[10] even though the main channel for the quenching of $Hg(6^3P_1)$ is this fine-structure process (1) for both of the Hg−N_2 and Hg−CO systems.

The intramultiplet process for Hg−N_2 is often explained by near resonant electronic-to-vibrational (E−V) energy transfer mechanism accompanied by simultaneous vibrational excitation:

$$Hg(6^3P_1) + N_2(^1\Sigma_g^+, v = 0, J) \rightarrow Hg(6^3P_0) + N_2(^1\Sigma_g^+, v = 1, J') \quad (2)$$

from the observation of the change in the lifetime of the metastable $Hg(6^3P_0)$ with intense resonance radiation at 253.7 nm, which enhances the reverse process of (2) to make the lifetime of $Hg(6^3P_0)$ effectively shorter.[11,12] This is an endoergic process by 564 cm^{-1}, and only the higher energy tail of the Boltzmann velocity distribution contributes to a relatively small cross section ($\sigma = 0.77$ A^2) at the room temperature.[10] However, Deech et al.[4] measured the quenching cross sections for $^{14}N_2$ and $^{15}N_2$ to observe an effect of the energy defect and found no isotope effect. This result seems to be inconsistent with the proposed near resonant E−V mechanism, because the cross sections for near resonant process must be sensitive to the energy defect of the process. The intramultiplet relaxation of the $Hg(6^3P_1)$−CO has also been explained by the same mechanism for N_2,[13]

$$Hg(6^3P_1) + CO(^1\Sigma^+, v = 0, J) \rightarrow Hg(6^3P_0) + CO(^1\Sigma^+, v = 1, J') \quad (3)$$

whose energy defect is 376 cm^{-1}. Even though this energy defect for the process (3) is smaller than that for the process (2), the process (3) requires that most of the translational and rotational energy is transferred to the vibrational motion of CO. Furthermore, it would be difficult to attribute the large difference in the cross sections, $\sigma(CO)/\sigma(N_2) \approx 30{:}1$, only to the change of the energy defect from 564 to 376 cm^{-1}. Thus, more experimental and theoretical efforts are needed to understand the dynamics of the collisional intramultiplet transitions with N_2 and CO.

Although the cross sections determined in previous experiments[1−7] are important basic data to study these inelastic or reactive processes, it is difficult to get detailed dynamical information from such data. Measurements of the translational energy dependence of the cross sections would give us further important information for understanding the dynamical aspects of these processes. In gas cell experiments, the energy depend-

* Corresponding author. E-mail: mo@rism.tohoku.ac.jp.

10.1021/jp984185w CCC: $18.00
Published on Web 03/06/1999

ence can be monitored by varying the temperature of the system. For Hg−N_2, the temperature dependence of the quenching cross section was measured over the range between 325 and 525 K by Matland.[5] However, the change of the temperature induces additional complexities by varying the rovibrational temperature of the target molecules simultaneously so that the pure translational energy effect on the cross section cannot be separated. Therefore, the present experiment has been carried out to observe the translational energy dependence of the relative cross sections for both the Hg(6^3P_1)−N_2 and Hg(6^3P_1)−CO collisions using a seeded beam method.

This paper is organized as follows. After a brief description of the experimental procedure including measurements of the velocity distributions of Hg, the results of a crossed beam experiment are presented for a collision energy range between 800 and 3750 cm^{-1}. We have found that the target molecules N_2 and CO give opposite energy dependences in this energy range. This is discussed based on the characteristic features of the intermolecular potentials of Hg−N_2 and Hg−CO. An energy threshold for the appearance of Hg(6^3P_0) around 900 cm^{-1} has been observed for Hg−N_2. This suggests the simultaneous vibrational excitation of N_2 from $v = 0$ to 1. Results of a beam-gas experiment are then presented and compared with those in the crossed-beam experiment to examine the effect of the rotational temperature of the target molecules. The different results of these two experiments for Hg−N_2 reveal the importance of initial rotational motion of the quencher molecule N_2. In addition, absolute values of the cross sections under the beam-gas conditions have been estimated by comparing these experimental results with absolute values of the partial cross sections determined in the gas cell experiment at room temperature.[8]

II. Experimental Section

A. Overview. The experimental arrangement used in this study is similar to that described in the preceding paper[14] (referred to as paper 1 in this article) and only a brief description will be given here. Experiments were performed under crossed-beam and beam-gas conditions combined with a laser pump−probe method. The crossed-beam apparatus described in paper 1 was used in both crossed-beam and beam-gas experiments. A pulsed valve operated with 10 Hz was used to generate the Hg atomic beam seeded in various rare gases or their mixtures with a backing pressure of 1 atm. The velocity of the seeded Hg beam was changed by altering the seeding rare gas from He to Kr to obtain the relative cross section as a function of the translational energy between 800 and 3750 cm^{-1} in the crossed-beam experiment and between 450 and 3350 cm^{-1} in the beam-gas experiment. In the crossed-beam experiment, a supersonic beam of the target gas (N_2 or CO) was crossed with the seeded Hg beam perpendicularly at the scattering center of the main chamber. In the beam-gas experiment, the Hg beam was directed into the main chamber filled with the molecular gas (N_2 or CO) at a pressure about 3×10^{-4} Torr to ensure single-collision conditions in the scattering region. The laser pump−probe scheme to observe the fine-structure process (1) is illustrated in Figure 1. The pump laser at 253.7 nm excited the ground-state Hg atoms to the 6^3P_1 state and the probe laser monitored the product Hg(6^3P_0) by measurements of laser-induced fluorescence (LIF). Fluorescence signal from the 6^3P_1 state to the ground state was also detected simultaneously to monitor the density of the excited Hg(6^3P_1) in the scattering region. This fluorescence signal was used to normalize the intensity of the product Hg($^3P_0$) monitored with the probe laser.

B. Estimation of Polarization-Independent Relative Cross Sections. At the lower collision energies covered in the present

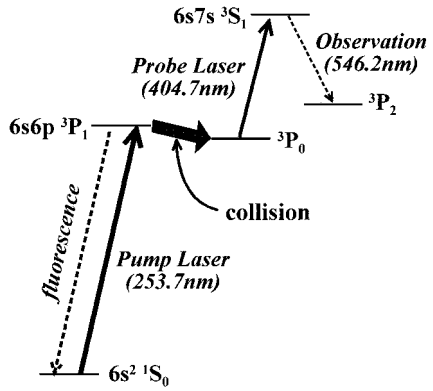

Figure 1. Energy diagram of mercury illustrating the excitation and detection scheme with their transition wavelengths.

study, the densities of the Hg in the seeded atomic beam were very low due to the use of heavier seeding rare gases. We thus changed the pump laser power and the delay time between the pump and probe lasers to obtain more intense signals. The power of the pump laser was 3 or 4 times higher than that used in paper 1. This gave rise to a partial saturation of the Hg(6^3P_1−6^1S_0) transition and, therefore, reduced the polarization dependence of the observed cross section. The delay time between the pump and probe lasers was fixed at about 200 ns, which was 4 times longer than that used in the paper 1. With this delay time, the effect of a residual magnetic field also reduced the polarization dependence of the cross section significantly. The reduction of the polarization dependence induced by these two changes of the experimental conditions, however, was not a problem at all for the present purpose, because our aim was to measure the cross sections as a function of the translational energy, irrespective of polarization angle.

To obtain the polarization-independent cross section, one has to set the polarization angle of the pump laser at the magic angle (54.7°) with respect to the direction of the initial collision velocity. For this purpose, the polarization angle of the pump laser must be changed every time when the velocity of the Hg atoms in the seeded beam varies in the crossed-beam experiment, because the direction of the collision velocity in the laboratory frame varies as the change of the velocity of Hg. Moreover, the fluorescence intensity at 253.7 nm also depends on the polarization angle of the pump laser as explained in paper 1. Thus, we adopted the following approximate but simple approach to estimate the polarization-independent relative cross sections. We measured the relative cross section with the laboratory polarization angle (θ_{lab}) of the pump laser fixed at $\theta_{lab} = 0$ and 90°, where the origin of θ_{lab} was defined as the direction of the Hg beam. An average of these two cross sections was adopted to represent the polarization-independent cross section approximately. The relative cross section obtained in this way is proportional to $(\sigma_\perp + \sigma_{||})/2$, where $\sigma_\perp$ and $\sigma_{||}$ are the cross sections with perpendicular and parallel excitations of the pump laser polarization with respect to the initial collision velocity; i.e.,

$$\{\sigma(\theta_{lab} = 0°) + \sigma(\theta_{lab} = 90°)\}/2 = (\sigma_\perp + \sigma_{||})/2 \quad (4)$$

because the cross section $\sigma(\theta_{lab})$ depends on the laboratory polarization angle θ_{lab} as[14]

$$\sigma(\theta_{lab}) = \sigma_0[1 + \beta P_2(\cos(\theta_{lab} - \theta_0))] \quad (5)$$

where θ_0 is the direction of the initial collision velocity, β is the asymmetry parameter, $P_2(\cos(\theta))$ is the second-order Leg-

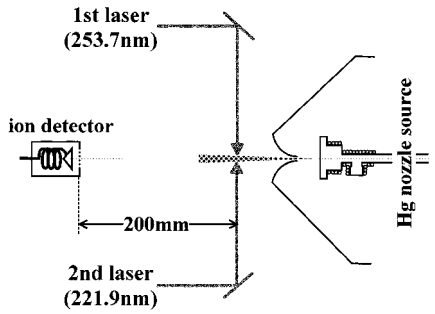

Figure 2. Schematic experimental setup for the TOF measurements of Hg to determine its velocity distribution

endre polynomial, and $\sigma_0 = (2\sigma_\perp + \sigma_\parallel)/3$ is the polarization-independent cross section. As stated above, the polarization dependence was small compared to that determined in the preceding study due to the effects of the saturation and the residual magnetic field under the present experimental condition. Indeed, $\beta = -0.2$ to -0.25 in this condition for Hg−N_2 at the collision energy of 3800 cm^{-1}, while it was -0.5 in the preceding study. Thus, the average cross section estimated in this study was a good approximation to the polarization-independent cross section σ_0. In the beam-cell experiment, the direction of the average collision velocity coincided with the direction of the Hg beam and θ_0 was always 0. Therefore, it was possible to estimate both the average cross section and the polarization-independent cross section independently, and they resulted in the same energy dependence within our experimental error.

C. Velocity Distribution of the Hg Atomic Beam. The normalized intensity I of the product Hg(6^3P_0) depends on the initial collision velocity v, its distribution $f(v)$, and the cross section $\sigma(v)$:

$$I = C\int_0^\infty \sigma(v)f(v)v\,dv \equiv C\sigma_{av}(v_{av})\int_0^\infty f(v)v\,dv \qquad (6)$$

where C is a constant, $\sigma_{av}(v_{av})$ is defined as an velocity-averaged cross section, and v_{av} is the average initial collision velocity calculated by

$$v_{av} = \int_0^\infty f(v)v\,dv \qquad (7)$$

In the present experiment, we have obtained the relative values of the velocity-averaged cross section $\sigma_{av}(v_{av})$ estimated by eq 6 as a function of the relative translational energy corresponding to the average velocity v_{av}. Since the velocity distribution in the crossed-beam experiment has a sharp peak at $v = v_{av}$, the $\sigma(v_{av})$ is essentially equal to the velocity-averaged cross section $\sigma_{av}(v_{av})$. However, in the beam-gas experiment, the relative velocity has a broad distribution due to the thermal distribution of the target molecules. Accordingly, the velocity-averaged cross section $\sigma_{av}(v_{av})$ sometimes deviates from the true cross section $\sigma(v_{av})$ significantly, as will be shown in the following section.

Theoretical estimation of the velocity distribution of atoms and molecules in a supersonic molecular beam is well established, and simple semiempirical equations can be used to determine the velocity distribution.[15] However, it is difficult to estimate the correct value of the velocity of Hg seeded in light rare gas atoms, because the Hg atoms are much heavier than these rare gas atoms and the velocity slip of Hg in the seeded beam must therefore be large. Thus, we have determined the velocity distribution of the Hg seeded in the rare gas atoms directly by applying a Rydberg time-of-flight (TOF) method.[16] Figure 2 shows the scheme of the TOF measurements. The first laser radiation at 253.7 nm excited the Hg atoms to the 6^3P_1 state, and then, the second laser at 221.9 nm excited the 6^3P_1 state to a high Rydberg state of Hg (n^3D_J, $n = 26$). The Rydberg atoms travelled over a distance of 200 mm as a neutral atom and then reached a box with an ion detector (Murata Ceratron-E), where they were field ionized and detected. Figure 3 shows the velocity distributions of the Hg seeded in various rare gases at the stagnation pressures of 1atm. The center velocity changes from about 440 to 1740 m/s and this allows us to measure translational energy dependence over a wide range of collision energies. The velocities of the Hg seeded in light rare gases such as He and the mixture of 20% Ne in He were found to deviate from the theoretical predictions (by more than 10% of the velocity for He) due to the velocity slip of the heavy Hg, while only small deviations were observed for heavier seeding gases such as Ar and Kr. The observed velocity distributions were least-squares fit to the shifted-Gaussian function $g(v)$:

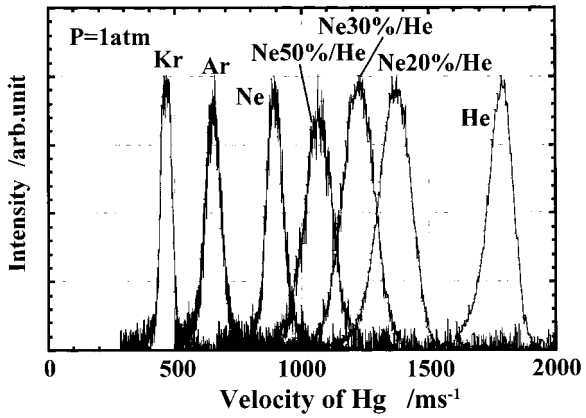

Figure 3. Velocity distributions of the Hg seeded in various rare gases. The stagnation pressure in the pulsed valve is kept at 1 atm.

TABLE 1. Parameters for the Velocity Distributions of the Hg Atoms Seeded in Rare Gases, Which Are Least-Squares Fit to the Shifted Boltzman Function (eq 2)

seeding gases	v_0 (m/sec)	δ (m/sec)
He	1740	70
20%Ne/He	1370	95
30%Ne/He	1240	90
50%Ne/He	1060	70
Ne	870	60
Ar	630	40
Kr	440	35

$$g(v) = A\exp(-(v - v_0)^2/\delta^2) \qquad (8)$$

Table 1 shows the center velocity v_0 and the width δ for each of the seeding rare gases used in this study. The function $g(v)$ was used to estimate the velocity distribution $f(v)$ to evaluate the average translational energy and the average collision velocity v_{av} in the crossed-beam and beam-gas experiments.

III. Results and Discussion

A. Crossed-Beam Experiment. Figure 4 shows the relative cross sections for the fine-structure changing process (1) in collisions with N_2 and CO as a function of the relative translational energy between 800 and 3750 cm^{-1} under crossed beam conditions. Since N_2 and CO have the same mass number and similar properties such as polarizability and viscosity, we assume that the density and velocity in the molecular beam are almost the same for both N_2 and CO when the pulsed valve is operated under the same conditions. From the theoretical

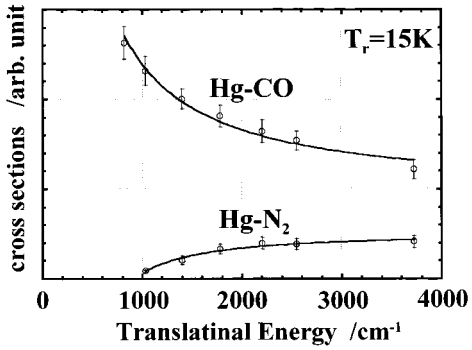

Figure 4. Translational energy dependences of the relative cross sections for Hg−N_2 and CO under the crossed-beam condition.

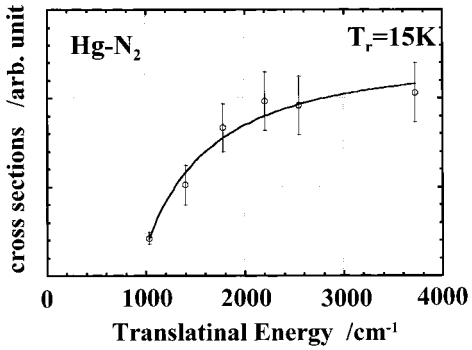

Figure 5. Translational energy dependence of the relative cross sections for Hg−N_2 measured in the crossed-beam experiment.

equations of molecular beams,[15] the velocities of N_2 and CO are estimated to be 770 m/s, and this value is used to estimate the relative translational energies and the collision velocities. The ratio of the cross section of the Hg−N_2 system to that of the Hg−CO system has been, therefore, determined by comparing the LIF intensities between the two systems without further corrections of the density and velocity of the target molecules. Figure 4 clearly exhibits quite different energy dependences for these two system. The cross section decreases with the increase of the translational energy for Hg−CO while it increases for Hg−N_2. Furthermore, the cross sections for Hg−N_2 and Hg−CO show an almost flat energy dependence near the highest energy studied. The energy dependence for Hg−N_2 in Figure 4 is expanded and shown in Figure 5. As the translational energy decreases, the cross section rapidly falls to indicate an energy threshold around 900 cm^{-1}.

Figure 6 shows qualitative one-dimensional potential curves of the Hg−N_2 system relevant to the fine-structure process (1). Since the anisotropic parts of the Hg−N_2 potential surfaces are assumed to be small in the region of interest due to the spherical-like electronic character of N_2, the one-dimensional potential curves must be similar to the spherical parts of the potential surfaces. Therefore, we explain the results of Hg−N_2 by using these one-dimensional potential curves. The process is considered to occur via the nonadiabatic $\tilde{A} \rightarrow \tilde{a}$ and/or $\tilde{B} \rightarrow \tilde{a}$ transitions,where the $\tilde{A}$ and $\tilde{B}$ states correlate to the initial state $Hg(6^3P_1)$ and the $\tilde{a}$ state to the product state $Hg(6^3P_0)$ at the infinite nuclear separation between the $Hg(6^3P_J)$ and N_2 ($X\ ^1\Sigma_g^+$). The one-dimensional potential parameters of the $\tilde{A}$ and $\tilde{B}$ states have already been determined by spectroscopic studies of the Hg−N_2 van der Waals (vdW) molecule,[17,18] but those of the $\tilde{a}$ state have not been determined. Therefore, we calculated the one-dimensional potential curve of the $\tilde{a}$ state by a simple semiempirical effective Hamiltonian method[19−22] in which the spin−orbit coupling of the $Hg(6^3P_J)$ and the potential curves

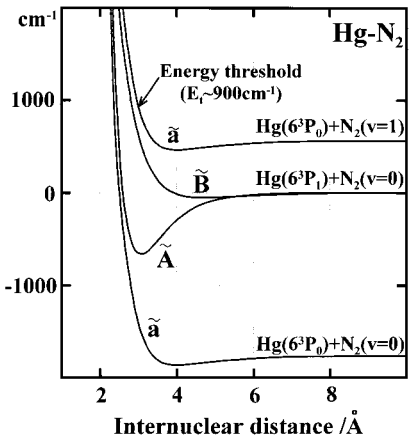

Figure 6. Intermolecular potentials of the $\tilde{A}$, $\tilde{B}$, and $\tilde{a}$ states of Hg−N_2. The potential of the $\tilde{a}$ state is calculated by the semiempirical method described in the text. For the $\tilde{a}$ state, two molecular potentials correlating with the $Hg(6^3P_0) + N_2$ ($v = 0$) and N_2 ($v = 1$) are both presented.

of the $\tilde{A}$ and $\tilde{B}$ states were used.[23] In this semiempirical calculation, the repulsive part of the $\tilde{B}$ state potential was slightly modified so as to facilitate this calculation; if not modified, the calculated potential of the $\tilde{a}$ state diverged at $R \approx 3.5$ Å. The previous vdW experiments determined the potential parameters only in an attractive well of the potential, and the repulsive wall of the $\tilde{B}$ state potential was too steep when these parameters were used to calculate that part of the $\tilde{B}$ state potential. Figure 6 includes the potential curve associated with the product $Hg(6^3P_0)$ and the vibrationally excited state of N_2 ($v = 1$). This curve is calculated approximately by adding one vibrational quantum of N_2 ($X\ ^1\Sigma_g^+$) to the calculated $\tilde{a}$ state potential.

As seen in Figure 6, the $\tilde{A}$ state approaches to the $\tilde{a}$ state with N_2 ($v = 0$) around the repulsive wall of its potential curve much more closely than the $\tilde{B}$ state. As discussed in paper 1, however, the nonadiabatic $\tilde{A}$−$\tilde{a}$ transition is almost forbidden for Hg−N_2 compared with the $\tilde{B} \rightarrow \tilde{a}$ transition due to the small anisotropy of electrostatic interaction between $Hg(6^3P_J)$ and N_2 ($X\ ^1\Sigma_g^+$). Nevertheless, the energy gap between the $\tilde{B}$ and $\tilde{a}$ state curves in Figure 6 is too large for the $\tilde{B}$−$\tilde{a}$ transition to occur at the present collision energies (≥900 cm^{-1}). In contrast, the $\tilde{B}$ state potential approaches to the $\tilde{a}$ state potential with N_2 ($v = 1$) closely at a collision energy around 900 cm^{-1}, as indicated in Figure 6. Hence, our observation of the threshold at this collision energy strongly suggests that the nonadiabatic $\tilde{B}$−$\tilde{a}$ transition for Hg−N_2 is located at the repulsive wall of the $\tilde{B}$ state potential and leads to the simultaneous vibrational excitation of N_2 ($v = 1$) as suggested in previous studies.[11,12]

For Hg−CO, we have no experimental data on the potential surfaces of this system. However, the observed negative translational energy dependence (Figure 4) indicates that the nonadiabatic transition is located at an attractive part of the $\tilde{A}$ or/and $\tilde{B}$ state potential and that the well depth is significantly large. As discussed in paper 1, despite the considerable contribution from the nonadiabatic transition via the $\tilde{A}$ state, the main pathway is still that via the $\tilde{B}$ state. Therefore, the $\tilde{B}$ state of Hg−CO must have a much deeper attractive well than that of Hg−N_2, which has a very shallow well ($D_e \approx 50$ cm^{-1}) for the $\tilde{B}$ state as shown in Figure 6. Indeed, the ab initio calculation of this system indicates that the potentials of the $\tilde{a}$ and $\tilde{B}$ states as well as the $\tilde{A}$ state are strongly bound with deep wells ($D_e = 5000-7000$ cm^{-1}) when Hg approaches on the C side of CO.[24] Furthermore, this calculation shows that these three potentials approach each other closely near the

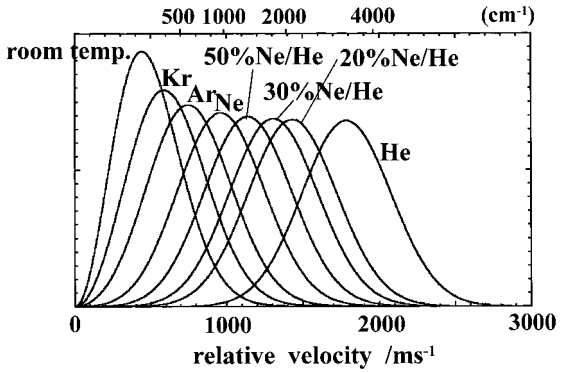

Figure 7. Relative velocity distribution for the Hg−N_2 and CO systems in the beam-gas experiment for each of the seeding rare gases in the Hg atomic beam.

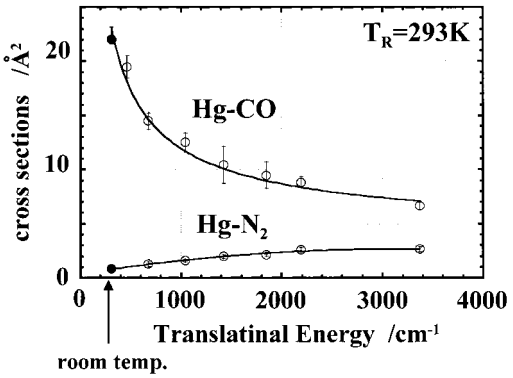

Figure 8. Translational energy dependences of the cross sections for Hg−N_2 and CO measured in the beam-gas experiment. The closed circles show the absolute values of the cross sections determined in gas cell experiments at room temperature.[8]

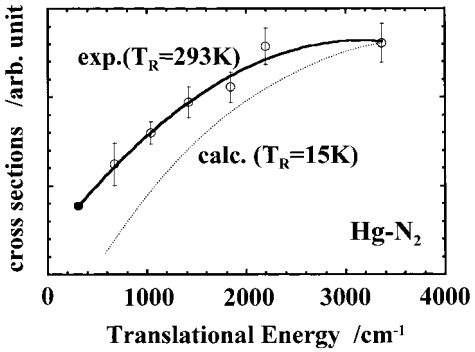

Figure 9. Translational energy dependence of the cross sections for Hg−N_2 measured in the beam-gas experiment (T_R = 293 K). The dotted line shows the calculated velocity-averaged cross section of the crossed-beam experiment at T_R = 15 K (see text).

bottom of the wells, around $R \approx 2.8$ Å. Hence, the negative energy dependence observed in this experiment for Hg−CO can be attributed to these strongly attractive potentials of both the $\tilde{B}$ state and the $\tilde{A}$ state, and the localization of the nonadiabatic transitions within these wells.

In the present explanation, the possibility of vibrational excitation of CO from $v = 0$ to 1 is excluded. However, the anisotropy of the intermolecular potentials for Hg−CO are large and we cannot ignore the possibility that the $\tilde{a}$ state potential with CO ($v = 1$) approaches the $\tilde{B}$ state or the $\tilde{A}$ state potentials at bent configuration within their attractive wells. Therefore, we do not have any definite conclusion on the possibility of the vibrational excitation of CO from our present experiment.

B. Beam-Gas Experiment. The cross section for the fine-structure transition of the Hg−N_2 collisions has been determined at room temperature in the gas cell experiments,[5,10] where the relative translational energy averaged over the Boltzmann distribution was about 300 cm^{-1}. This average translational energy is much less than the energy threshold (~900 cm^{-1}) obtained in the present crossed-beam experiment. Thus, the observation of this threshold seems to be inconsistent with the observation in the gas cell experiment. However, we have to consider two factors in comparing these two results. One is the difference in the rovibrational temperature of the target molecules (N_2 and CO), and the other is the difference in the relative velocity distributions. Vibrational frequencies of N_2 and CO are so high that we can ignore the population of vibrationally excited states of N_2 and CO in both the experiments, and therefore, only the rotational temperature (T_R) is taken into account. In the crossed-beam experiment, the target molecules are rotationally cold ($T_R \approx 15$ K in the present experiment[14]) and the velocity distribution is narrow and localized at the average collision velocity v_{av}. In the gas cell experiment, however, the rotational temperature is equal to room temperature ($T_R \approx 293$ K) and the relative velocity distribution is broad. To elucidate the origin of the difference in these two experiments, we have carried out beam-gas experiments, where the rotational temperature of the target molecules (N_2 or CO) is the same as that in the gas cell experiment at the room temperature and the relative velocity has a broad distribution like a Boltzmann velocity distribution in the gas cell experiment. Using the seeded Hg beam, we have measured the velocity-averaged cross sections as a function of the average translational energy under the beam-gas conditions and compared them with the results of the crossed-beam experiment.

Figure 7 shows the relative velocity distributions $f(v)$ of the Hg−N_2 and Hg−CO systems for the present beam-gas experiment. We have calculated them by using a Boltzmann distribution of the velocity of N_2 or CO at room temperature ($T = 297$ K) and the measured velocity distribution $g(v)$ of the seeded Hg beam summarized in Table 1. Since N_2 and CO have almost the same velocity distributions as stated in the previous section, only one set of the velocity distribution in Figure 7 represents both of the distributions for the Hg−N_2 and Hg−CO systems. The average collision velocity v_{av} is calculated by eq 7 from the velocity distribution $f(v)$ in Figure 7. The velocity-averaged cross section $\sigma_{av}(v_{av})$, which is obtained as I/v_{av} from the normalized signal intensity I, is shown in Figure 8 as a function of the translational energy averaged over the distributions $f(v)$. The energy dependences for Hg−N_2 and Hg−CO are similar to those of the crossed-beam experiments (Figures 4 and 5) except for the slope for Hg−N_2 at lower collision energies. The translational energy dependence for Hg−N_2 in Figure 8 is enlarged in Figure 9. The cross section in the beam-gas experiment shows a slower dependence than that in the crossed beam experiment (Figure 5). In addition, the cross section for Hg−N_2 has no clear threshold and can be extrapolated to the translational energy corresponding to the room temperature as indicated in Figure 8. The ratio of the cross section of Hg−CO relative to that of Hg−N_2 is extrapolated to about 30 at the average translational energy at room temperature. This ratio is in good agreement with that obtained in the gas cell experiment.[8] We can therefore estimate the absolute values of the cross sections by comparing these extrapolated relative values with the experimentally determined absolute values at room temperature[8] which are indicated by closed circles in Figures 8 and 9.

For direct comparison of the results of these two experiments for Hg−N_2, we calculated the translational energy dependence of the velocity-averaged cross section in the crossed-beam

experiment ($T_R = 15$ K) by eq 6, corresponding to the relative velocity distribution realized in the beam-gas experiment in Figure 7; that is, we substituted the relative cross section determined by the crossed-beam experiment in Figure 5 for $\sigma(v)$ in eq 6 and the velocity distribution function of the beam-gas experiment in Figure 7 for $f(v)$ in eq 6. The calculated cross section $\sigma_{av}(v_{av})$ at $T_R = 15$ K is shown in Figure 9 by a dotted line as a function of the translational energy and is compared with the cross sections $\sigma_{av}(v_{av})$ at $T_R = 297$ K obtained in the beam-gas experiment. After taking the effect of the relative velocity distribution into account, the difference of these two curves depends only on the initial rotational energy of N_2. As seen in Figure 9, the calculated cross section $\sigma_{av}(v_{av})$ at $T_R = 15$ K has a threshold around 500 cm^{-1} while the cross section in the beam-gas experiment at $T_R = 293$ K does not show a clear threshold. This means that the change of the rotational temperature from 15 to 293 K gives rise to the shift of the threshold to the lower energy region. Thus, we conclude that (i) the rotational energy of N_2 has a role in compensating the energy defect, and/or (ii) the nonadiabatic coupling responsible for this fine-structure transition is associated with the rotational motion of N_2 and the higher rotational temperature of N_2 enhances the nonadiabatic transition, especially at lower collision energies.

As mentioned above, the cross section for Hg−CO is about 30 times larger than that for Hg−N_2 at room temperature in the gas cell experiment,[8] and we attribute this large difference mainly to the difference of the region of their molecular potentials where the nonadiabatic transitions occur. This relates to the range of impact parameters for these nonadiabatic transitions; that is, for Hg−N_2, collisions with only small impact parameters can lead to the nonadiabatic transition, but for Hg−CO, collisions with large impact parameters can contribute to the nonadiabatic transition at the low collision energies corresponding to the room temperature. At collision energies larger than 3000 cm^{-1}, however, the cross sections for both the Hg−N_2 and Hg−CO systems show almost flat energy dependences, as shown in Figures 4 and 8. At these collision energies, the cross section for Hg−CO is only about 3 times larger than that for Hg−N_2. This difference of a factor of 3 can be attributed to the difference in the magnitude of the nonadiabatic coupling which is probably associated with the differnce in the anisotropy of the electrostatic interactions between the Hg−N_2 and Hg−CO systems, as discussed in paper 1.

In conclusion, we have measured the translational energy dependences of the relative cross sections for the fine-structure transitions of Hg(6^3P_1−6^3P_0) in collisions with N_2 and CO. The observed energy dependence for Hg−N_2 shows that the nonadiabatic transition responsible for this fine-structure process occurs at the repulsive wall of the $\tilde{B}$ state potential, while that for Hg−CO suggests that the region of the nonadiabatic transition is located within the well of the strongly bound potential for the $\tilde{B}$ state as well as that for the $\tilde{A}$ state. The energy dependence for Hg−N_2 also shows the existence of an energy threshold for the appearance of Hg(6^3P_0) around 900 cm^{-1}, which indicates the possibility of simultaneous vibrational excitation of N_2 ($v = 1$). We have also estimated the absolute values of the cross sections for Hg−N_2 and CO under beam-gas conditions. Finally, we have shown that the initial rotational energy of N_2 enhances the cross section of this fine-structure process, particularly at the lower collision energies.

Acknowledgment. The present study is supported in part by the Grant-in-Aid for Scientific Research (08740438 and 09740412) from the Ministry of Education of Japan.

References and Notes

(1) King, D. L.; Setser, D. W. *Annu. Rev. Phys. Chem*. **1976**, *27*, 407 and references cited therin.
(2) Breckenridge, W. H.; Umemoto, H. *Adv. Chem. Phys*. **1982**, *50*, 325 and references therein.
(3) Cvetanovic, R. J. *Prog. React. Kinet.* **1964**, *2*, 39.
(4) Deech, J. S.; Pitre, J.; Krause, L. *Can. J. Phys.* **1971**, *49*, 1976.
(5) Matland, C. G. *Phys. Rev*. **1953**, *92*, 637.
(6) Michael, J. V.; Suess, G. N. *J. Phys. Chem*. **1974**, *78*, 482.
(7) Gleditsch, S. D.; Micheal, J. V. *J. Phys. Chem*. **1975**, *79*, 409.
(8) Phillips, L. F. *Acc. Chem. Res*. **1974**, *7*, 135.
(9) Campbell, J. M.; Strausz, O. P.; Gunning, H. E. *J. Am. Chem. Soc*. **1973**, *95*, 740.
(10) Horiguchi, H.; Tsuchiya, S. *Bull. Chem. Soc. Jpn*. **1977**, *50*, 1661.
(11) Horiguchi, H.; Tsuchiya, S. *J. Chem. Soc., Faraday. Trans. 2* **1975,** *71*, 1164.
(12) Degani, J.; Rosenfeld, E.; Yatsiv, S. *J. Chem. Phys*. **1978**, *68*, 4041.
(13) Callear, A. B.; Wood, P. M. *Trans. Faraday Soc*. **1971**, *67*, 2862.
(14) Okunishi, M.; Hashimoto, J.; Chiba, H.; Ohmori, K.; Ueda, K.; Sato, Y. *J. Phys. Chem.* **1999**, *103*, 1734.
(15) Miller, D. R. In *Atomic and Molecular Beam Method*; Scoles, G, Ed.; Oxford University Press: New York, 1988.
(16) Schnieder, L.; Seekamp-Rahn, K.; Liedeker, F.; Steuwe, H.; Welge, K. H. *Faraday Discuss. Chem. Soc*. **1991**, *91*, 259.
(17) Yamanouchi, K.; Isogai, S.; Tsuchiya, S.; Duval, M.-C.; Jouvet, C.; d'Azy, O. B.; Soep, B. *J. Chem. Phys*. **1988**, *89*, 2975.
(18) Fuke, K.; Saito, T.; Nonose, S.; Kaya, K. *J. Chem. Phys*. **1987**, *86*, 4745.
(19) Devdariani, A. Z.; Zagrebin, A. L. *Khim Fiz*. **1986**, *5*, 147.
(20) Zagrebin, A. L.; Lednev, M. G.; Tserkovnyi, S. I. *Opt. Spectrosc*. **1993**, *74*, 14.
(21) Zagrebin, A. L.; Tserkovnyi, S. I. *Opt. Spectrosc*. **1993**, *75*, 161.
(22) Kurosawa, T.; Ohmori, K.; Chiba, H.; Okunishi, M.; Ueda, K.; Sato, Y.; Devdariani, A. Z.; Nikitin, E. E. *J. Chem. Phys*. **1998**, *108*, 8101.
(23) In the present calculation, an off-diagonal term of the spin−orbit coupling between the singlet (6^1P_1) and triplet (6^3P_1) states of Hg is neglected to simplify the calculation procedure since inclusion of this off-diagonal term gives almost no effect on the calculated potentials themselves.
(24) Kato, S.; Jaffe, R. L.; Komornicki, A.; Morokuma, K. *J. Chem. Phys*. **1983**, *78*, 4567.